

Article

Tuning the electrical parameters of p-NiO_x based Thin Film Transistors (TFTs) by pulsed laser irradiation

Poreddy Manojreddy¹, Srikanth Itapu^{2*}, Jammalamadaka Krishna Raval³ and Selvendran S⁴

¹ Department of ECE, CVR College of Engineering, Hyderabad, India; manojreddy0359@gmail.com

² School of Electronics Engineering (SENSE), Vellore Institute of Technology (VIT), Vellore, India; srikanth.itapu@rockets.utoledo.edu

³ School of MS, University of Hyderabad, India; 19mbmb12@uohyd.ac.in

⁴ School of Electronics Engineering (SENSE), Vellore Institute of Technology (VIT), Chennai, India; selvendranc@aol.com

* Correspondence: srikanth.itapu@rockets.utoledo.edu;

Abstract: We utilized laser irradiation as a potential technique in tuning the electrical performance of NiO_x/SiO₂ thin film transistors (TFTs). By optimizing the laser fluence and the number of laser pulses, the TFT performance is evaluated in terms of mobility, threshold voltage, on/off current ratio and subthreshold swing, all of which were derived from the transfer and output characteristics. The 500 laser pulses irradiated NiO_x/SiO₂ TFT exhibited an enhanced mobility of 3 cm²/V-s from a value of 1.25 cm²/V-s for as-deposited NiO_x/SiO₂ TFT. The laser-irradiated NiO_x material likely has a significant concentration of defect gap states, which could also be involved in light absorption processes. Second, and more importantly, the excess energy that the photogenerated charge carriers possess (due to the significant difference between the photon energy and the bandgap of NiO_x), combined with the very high light intensity, would result in complex thermal and photo thermal changes thus resulting in an enhanced electrical performance of p-type NiO_x/SiO₂ TFT structure.

Keywords: Laser irradiation, p-type NiO, SiO₂ layer, Thin film transistor

1. Introduction

Over the last few years, metal oxide semiconductors have received considerable attention for the applications in thin-film transistors (TFTs) because of their superior physical properties [1]. Extensive research on n-type oxide semiconductors (for example, Indium Gallium Zinc Oxide (InGaZnO), Zinc Oxide (ZnO), and Indium Oxide (In₂O₃)) resulted in industry-specific high-performance oxide TFTs. It is imperative to develop p-type substitutes for the development of next-generation transparent electronics which would enable the development of complementary metal-oxide semiconductor (CMOS) circuits [2], [3]. Few p-type semiconductors such as compounds, Tin Oxide (SnO), Copper Oxide (Cu₂O), and Nickel Oxide (NiO_x), have been demonstrated and incorporated into transistors as the p-type channels. Meanwhile, high performance p-type oxide remains to be a challenging work due to the localized 2p orbitals in the valence band maximum (VBM), the deep VBMs (5–8 eV), and self-compensation by donors [4]. It is well known that stoichiometric deviation alters the electronic structure, and oxygen vacancy causes the formation of sub-gap defects and donor states in many oxides. Therefore, a trade-off between the stoichiometry and the mechanisms employed for defect termination processes are determine the extent of electrical performance of the p-type oxide transistors.

Among various p-type oxide candidates, NiO_x is an interesting and promising material due to its superior optical transparency, chemical stability and wide range of applicability vis-à-vis, rectifying diodes [5], p-type Metal Insulator Semiconductor (MIS) structures [6], tin whisker growth mitigation by NiO sublayers [7], etc. The stoichiometric

NiO is a Mott insulator with a conductivity of 10^{-13} S/cm, while nonstoichiometric NiO_x is a wide-band-gap p-type semiconductor. The p-type conductivity of NiO_x originates from two positive charge compensation which favors Ni^{2+} vacancies [8]. Several methods have been used for growing NiO films, including sputtering [9-12], e-beam evaporation [13, 14], chemical and plasma-enhanced chemical vapor method [15], sol-gel [16], pulsed laser deposition [17], spray pyrolysis [18, 19]. Sputtering, which is a type of physical vapor deposition technique, is preferred due to its industrial scalability. However, the composition and electrical conductivity of sputtered films are far from equilibrium [20, 21]. Lattice defects are not well-defined in NiO films with high oxygen content [22]. Some studies used working gas and thermal annealing to adjust the film composition and found that the lattice parameter increased with increasing oxygen content, thus resulting in oxygen interstitials as the dominant defects. However, the lattice parameter may not be appropriate to determine the dominant mechanism. On the other hand, the dynamics of interstitials/vacancies created due to laser irradiation are little discussed regarding non-stoichiometric NiO films [23].

Similarly, laser irradiation has been used for modifying intrinsic properties of metallic [24, 25], semiconducting [26-29], superconducting [30], multiferroic [31] and ceramic [32] thin films. In [33], the most frequently used high dielectric material, hafnium oxide (HfO_2) was subjected to irradiation by continuous wave laser with wavelength 355nm to analyze the temporal behavior of absorption annealing. In [34], post-deposition annealing of tin oxide (SnO_2) thin films by ultra-short laser pulses resulted in a change in refractive index and conductivity of the films. Significant modification in the stoichiometry, desorption of dopant atoms and adsorption of hydrogen atoms from the atmosphere were also observed. Crystallization of amorphous titanium oxide (TiO_2) by pulsed laser irradiation using an excimer laser is studied in [35]. Cadmium oxide (CdO) thin films deposited by sol-gel coating method were laser irradiated using a Q-switched Nd:YAG laser operating at its first and second harmonic wavelengths in [36]. An agglomeration of nanoparticles and variation in the bandgap, photoluminescence spectra with laser irradiation were observed. The structural, optical, luminescent and vibrational properties of zinc oxide (ZnO) under the influence of continuous-wave CO_2 laser irradiation were studied in [37]. In this work, we explore the effect of ultra-violet (UV) laser irradiation in tuning the properties of NiO thin films, thus enhancing the electrical performance of NiO based TFTs.

In [38], the low-temperature solution-processed p-type nickel oxide thin films along with an aqueous high-k aluminium oxide Al_2O_3 gate dielectric significantly improved the electrical performance of NiO_x TFT compared to those based on SiO_2 dielectric. The hole mobility was reportedly enhanced by 60 times from 0.07 to $4.4 \text{ cm}^2/\text{Vs}$. Similarly, ink-jet printed p-type NiO_x TFTs annealed at 280°C in [39], gave the best electrical performance with field-effect mobility of $0.78 \text{ cm}^2/\text{Vs}$, SS of 1.68 V/dec , on/off current ratio ($I_{\text{on}}/I_{\text{off}}$) of 5.3×10^4 with a 50nm Al_2O_3 insulator layer. By optimizing the annealing temperature, precursor concentration, source/drain electrodes, and dielectric material, the authors in [40] successfully achieved p-type NiO TFTs with remarkable mobility of $6.0 \text{ cm}^2/\text{Vs}$, excellent on/off current modulation ratio of 10^7 , as well as a good subthreshold swing of 0.13 V/decade at a low processing temperature of 250°C . Hence, from our previous works

[5-7, 23, 29], we propose the non-contact laser irradiation on sputter-deposited $\text{NiO}_x/\text{SiO}_2$ based TFTs as a potential technique to enhance the electrical parameters by tuning the laser fluence and a number of laser pulses. In this work, the relation between the number of laser pulses to the mobility of NiO_x , threshold voltage, on/off ratio and subthreshold swing of $\text{NiO}_x/\text{SiO}_2$ TFT device is also studied extensively.

2. Experimental Details

Nickel oxide films were deposited on SiO_2/Si substrate by reactive radio frequency (RF) magnetron sputtering from a 99.99% pure Ni target in an 80:20 oxygen–argon gas mixture at 300°C. We used multiple cleaning steps for our substrate. The cleaning procedure is as follows: wash in cleaning solution (Micro-90), then thoroughly rinse with DI water, followed by an ultra-sonication bath in methanol for 20-25 min, and, finally, ultra-sonication bath in ethanol for 20-25 min. In between these steps, the surfaces are rubbed with a lint-free wipe and blown dry with nitrogen. The thickness of the films was found to be about 100nm using spectroscopic ellipsometry studies [d]. Figure 1 depicts the layered structure of the NiO_x based TFT. Post-deposition, the TFT device is subjected to Nd:YAG laser irradiation laser operating at its fourth harmonic wavelength $\lambda = 266$ nm at room temperature (RT) with optimized laser fluence of 150 mJ/cm² for different number of pulses (Figure 2 (a-d)). The laser fluence is kept below a threshold for any observable physical damage/ablation. The mobility was obtained using a Hall effect measurement setup at room temperature with a magnetic field of 2500 G. The polycrystalline structure of the as-deposited NiO_x is verified on a Rigaku X-ray diffractometer with $\text{Cu K}\alpha$ radiation ($\lambda = 0.154\text{nm}$) and a Ni filter.

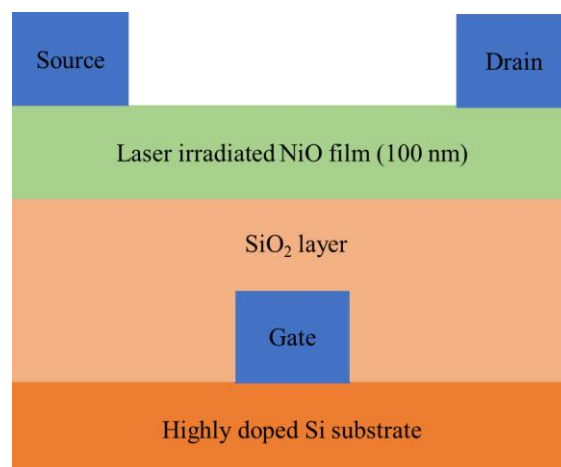


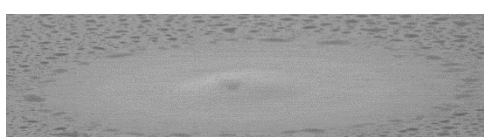
Figure 1. Layered structure of laser irradiated NiO_x based TFT (Staggered bottom gate TFT).



(a)



(b)



(c)

(d)

Figure 2. Scanning Electron Microscope images of laser-irradiated $\text{NiO}_x/\text{SiO}_2$ TFT (Scale: 1 inch = 10 μm). (a) Laser fluence of 125 mJ/cm^2 , (b) 150 mJ/cm^2 , (c) 175 mJ/cm^2 and (d) 200 mJ/cm^2 .

3. Results and Discussion

Dependence of number of laser pulses on electrical performance of the proposed TFT

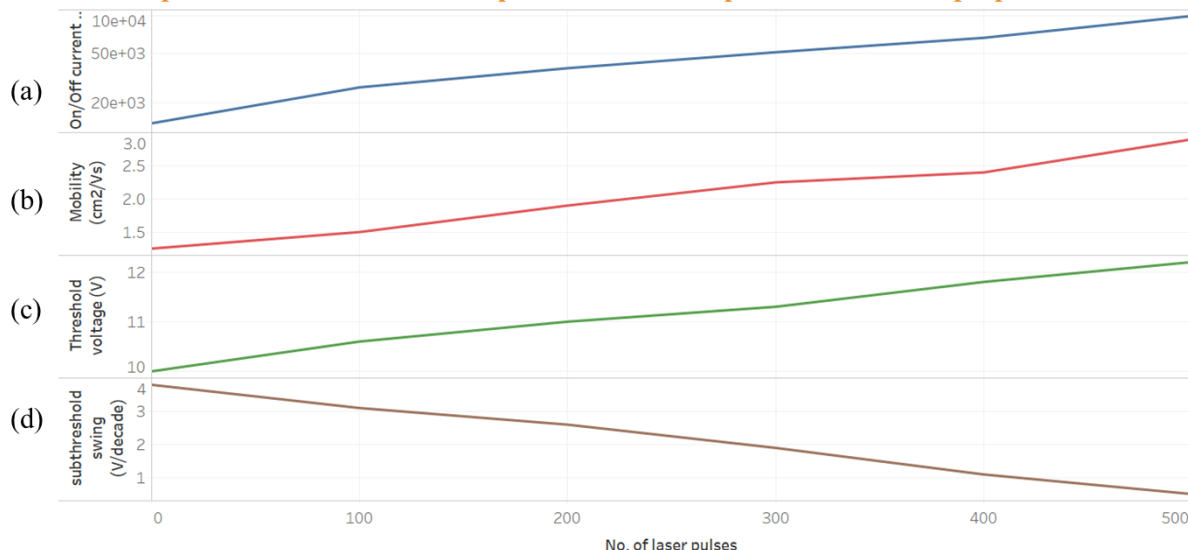


Figure 3. Dependence of number of laser pulses on (a) on/off current ratio, (b) mobility ($\text{cm}^2/\text{V}\cdot\text{s}$), (c) threshold voltage (V) and (d) subthreshold swing (V/decade)

Figure 3(a) represents the relationship between on/off current ratio and the number of laser pulses. The on/off current ratio $I_{\text{on}}/I_{\text{off}}$ is usually defined as the ratio of the maximum I_{DS} to the minimum I_{DS} (typically in saturation region), which can be extracted from the transfer characteristic curve. If the number of laser pulses increases from 0 to 500, then the ratio value constantly increases to 10^5 .

Figure 3(b) depicts the relationship between mobility and the number of laser pulses. Mobility is a parameter related to the efficiency of carrier transport in the material, which directly affects the maximum I_{DS} and the operating frequency of devices. Mobility is affected by several scattering mechanisms, including lattice vibrations, ionized impurities, grain boundaries, interface surface roughness, lattice strain and other structural defects, velocity saturation, and electron trapping [41]. Field-effect mobility which is the most widely used parameter to evaluate TFT performance, gradually increases from $1.25 \text{ cm}^2/\text{V}\cdot\text{s}$ to $3 \text{ cm}^2/\text{V}\cdot\text{s}$ as the number of laser pulses increases in steps of 100 pulses to 500 pulses.

Figure 3(c) establishes the relationship between the threshold voltage and the number of laser pulses. The threshold voltage (V_{TH}) is the value of V_{GS} when the accumulation layer or conductive channel formed near the dielectric layer/active layer interface in TFTs. Depending on the values of V_{TH} being negative or positive, the p-type TFT devices typically operate in

enhancement or depletion modes respectively. As the number of laser pulses increases from 0 to 500, then the value of threshold voltage increases slightly more than 12 V.

The subthreshold swing (SS) is an important parameter that indicates the switching efficiency of a transistor. The SS is directly related to the quality of the dielectric/semiconductor interface and defined as the inverse of the maximum slope of the transfer characteristic and reflected by the V_{GS} needed to increase the I_{DS} by one decade in the sub-threshold region. When the SS value is low, then the operation speed is high, and the power consumption is also low. As the number of laser pulses increases from 0 to 500, then the value of SS decreases from 3.8 to 0.65 V/decade (Figure 3(d)).

Furthermore, the associated $(I_{DS})^{1/2}$ and I_{GS} as a function of the V_{GS} were shown in Figure 4(a, b). It was found that the saturation drain-source current and the gate leakage current were $-40 \mu A$ and $-8 nA$, respectively, when the p-type NiO TFTs operated at a V_{DS} of $-10V$ and a V_{GS} of $-9V$. The associated on-to-off current ratio was 10^5 . The associated threshold voltage and subthreshold swing were $-4V$ and $0.56V/\text{decade}$, respectively.



Figure 4. Drain-source current and transconductance as a function of gate-source voltage of p-type NiO thin-film transistor.

The output characteristics of p-type NiO based TFT is divided into two main operating regions depending on the value of V_{DS} : linear and saturation regions. In linear region, V_{GS} controls the channel resistance thus accumulating charges uniformly in the channel. In saturation region, for a constant V_{GS} , I_{DS} is constant, which suggests lack of channel region due to depletion of charges in the accumulation layer. For the 500 pulses laser-irradiated $\text{NiO}_x/\text{SiO}_2$ TFT, the output characteristics are shown in Figure 5.

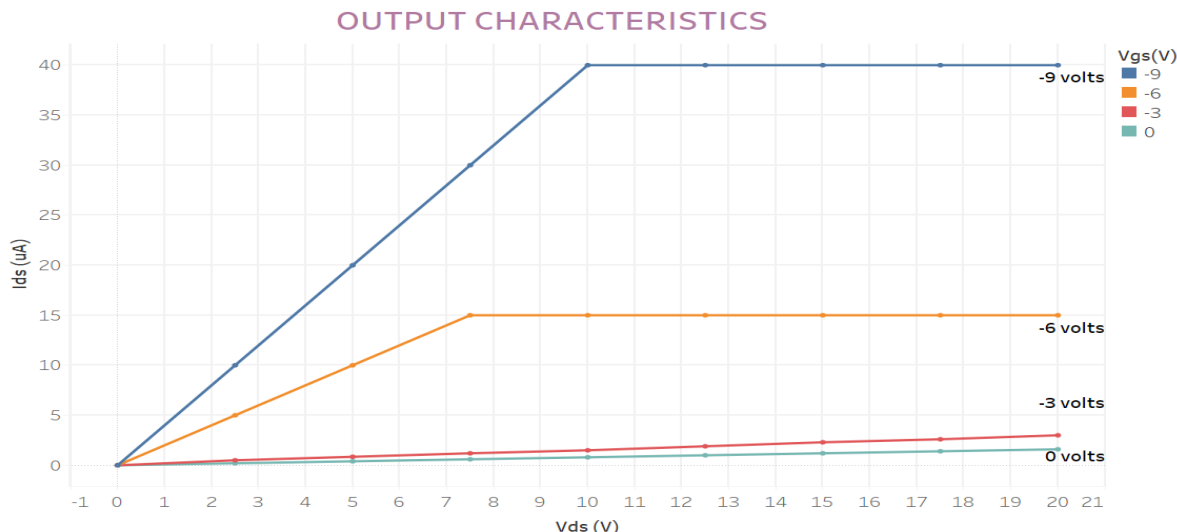


Figure 5. Drain source current- drain source voltage characteristics of the NiO TFT.

At constant V_{GS} of 0V, when voltage V_{DS} increases from 0V to 20V then the value of current I_{DS} increases from 0 μ A to 1.6 μ A. At constant V_{GS} of -3V, when voltage V_{DS} increases from 0V to 20V then the value of current I_{DS} increases from 0 μ A to μ A. At constant V_{GS} of -6V, when voltage V_{DS} increases from 0V to 7.5V then the value of current I_{DS} increases from 0 μ A to 15 μ A and remains constant up to 20V. Again, at constant V_{GS} of -9V when voltage V_{DS} increases from 0V to 10V then the value of current I_{DS} increases from 0 μ A to 40 μ A and remains constant up to 20V.

5. Conclusions

In this work, we studied the effects of laser irradiation in enhancing the electrical performance of p-type NiO_x TFT with SiO_2 as high-k dielectric layer. The mobility increased from $1.25 \text{ cm}^2/\text{V}\cdot\text{s}$ for as-deposited NiO_x thin film to $3 \text{ cm}^2/\text{V}\cdot\text{s}$ for 500 laser pulse irradiated sample. Similar enhancements were observed for laser irradiated sample in terms of the threshold voltage, subthreshold swing and the on/off current ratio. The plausible mechanism responsible for the reported phenomenon was that the excess energy, photogenerated charge carriers possess (due to the significant difference between the photon energy and the bandgap of NiO_x), combined with the very high light intensity, results in a complex thermal and photo thermal changes, thus enhancing the electrical performance of the TFT.

Author Contributions: “Conceptualization, P.M., S.I.; methodology, S.I., S.S.; software, J.K.R.; validation, P.M., S.I.; formal analysis, P.M., J.K.R.; investigation, S.I., S.S.; resources, S.I.; data curation, J.K.R.; writing—original draft preparation, P.M., S.I.; writing—review and editing, S.I., S.S.; visualization, J.K.R. All authors have read and agreed to the published version of the manuscript.”

Funding: This research received no external funding.

Data Availability Statement: In this section, please provide details regarding where data supporting reported results can be found, including links to publicly archived datasets analyzed or generated during the study. Please refer to suggested Data Availability Statements in section “MDPI Research Data Policies” at <https://www.mdpi.com/ethics>. You might choose to exclude this statement if the study did not report any data.

Acknowledgments: The authors would like to thank the department of Electrical Engineering and Computer Science (EECS) and the Center for Material Synthesis and Characterization (CMSC) at the University of Toledo for support to carry out this work.

Conflicts of Interest: The authors declare no conflict of interest.

References

1. Fortunato E., Barquinha P., and Martins R., "Oxide Semiconductor Thin-Film Transistors: A Review of Recent Advances," *Adv. Mater.*, **2012**, vol. 24, no. 22, pp. 2945–2986.
2. Pattanasattayavong P., Mottram A.D., Yan F., and Anthopoulos T.D., "Study of the Hole Transport Processes in Solution-Processed Layers of the Wide Bandgap Semiconductor Copper(I) Thiocyanate (CuSCN)," *Adv. Funct. Mater.*, **2015**, vol. 25, no. 43, pp. 6802–6813.
3. Martins R.F.P., Ahnood A., Correia N., Pereira L.M.N.P., Barros R., Barquinha P.M.C.B., Costa R., Ferreira I.M.M., Nathan A., and Fortunato E.E.M.C., "Recyclable, Flexible, Low-Power Oxide Electronics," *Adv. Funct. Mater.*, **2013**, vol. 23, no. 17, pp. 2153–2161.
4. Kim S.Y., Ahn C.H., Lee J.H., Kwon Y.H., Hwang S., Lee J.Y., and Cho H.K., "p-Channel Oxide Thin Film Transistors Using Solution-Processed Copper Oxide," *ACS Appl. Mater. Interfaces*, **2013**, vol. 5, no. 7, pp. 2417–2421.
5. Khan K., Itapu S. and Georgiev D.G., "Rectifying behavior and light emission from nickel oxide MIS structures", *MRS Advances*, **2016**, vol. 1, no. 49, pp. 3341-3347.
6. Khan K., Itapu S. and Georgiev D.G., "Negative differential resistance (NDR) behavior of nickel oxide (NiO) based metal-insulator-semiconductor structures", *J. Electro. Mat.*, **2020**, vol. 49, no. 1, pp. 333-340.
7. Borra V., Itapu S. and Georgiev D.G., "Sn whisker growth mitigation by using NiO sublayers", *J. Phys. D: Appl. Phys.*, **2017**, Vol. 50, no. 47, 475309, 2017.
8. J. R. Manders J.R., Tsang S.-W., Hartel M.J., Lai T.-H, Chen S., Amb C.M., Reynolds J.R., and So F., "Solution-Processed Nickel Oxide Hole Transport Layers in High-Efficiency Polymer Photovoltaic Cells," *Adv. Funct. Mater.*, **2013**, vol. 23, no. 23, pp. 2993–3001.
9. Sato H., Minami T., Takata S., and Yamada T., "Transparent conducting p-type NiO thin films prepared by magnetron sputtering," *Thin Solid Films*, **1993**, vol. 236, no. 1–2, pp. 27–31.
10. Chen S.C., Kuo T.Y., and Sun T.H., "Microstructures, electrical and optical properties of non-stoichiometric p-type nickel oxide films by radio frequency reactive sputtering," *Surf. Coatings Technol.*, **2010**, vol. 205, pp. S236–S240.
11. Chen H.-L, Lu Y.-M., and Hwang W.-S., "Characterization of sputtered NiO thin films," *Surf. Coatings Technol.*, **2005**, vol. 198, no. 1–3, pp. 138–142.
12. Reddy Y.A.K., "Influence of Growth Temperature on the Properties of DC Reactive Magnetron Sputtered NiO Thin Films," *Int. J. Curr. Eng. Technol.*, **2013**, vol. 2, no. 2, pp. 351–357.
13. Subramanian B., Mohammed Ibrahim M., Murali K.R., Vidhya V.S., Sanjeeviraja C., and Jayachandran M., "Structural, optoelectronic and electrochemical properties of nickel oxide films," *J. Mater. Sci. Mater. Electron.*, **2009**, vol. 20, no. 10, pp. 953–957.
14. Agrawal A., Habibi H.R., Agrawal R.K., Cronin J.P., Roberts D.M., CaronPopowich R., and Lampert C.M., "Effect of deposition pressure on the microstructure and electrochromic properties of electron-beam-evaporated nickel oxide films," *Thin Solid Films*, **1992**, vol. 221, no. 1–2, pp. 239–253.
15. Yeh W. and Matsumura M., "Chemical Vapor Deposition of Nickel Oxide Films from Bis- π -Cyclopentadienyl-Nickel," *Jpn. J. Appl. Phys.*, **1997**, vol. 36, no. Part 1, No. 11, pp. 6884–6887.
16. Guo W., Hui K.N., and Hui K.-S., "High conductivity nickel oxide thin films by a facile sol-gel method," *Mater. Lett.*, **2013**, vol. 92, pp. 291–295.
17. Tanaka M., Mukai M., Fujimori Y., Kondoh M., Tasaka Y., Baba H., and Usami S., "Transition metal oxide films prepared by pulsed laser deposition for atomic beam detection," *Thin Solid Films*, **1996**, vol. 281–282, pp. 453–456.
18. Reguig B.A., Khelil A., Cattin L., Morsli M., and Bernède J.C., "Properties of NiO thin films deposited by intermittent spray pyrolysis process," *Appl. Surf. Sci.*, **2007**, vol. 253, no. 9, pp. 4330–4334.

19. Kang J.-K and Rhee S.-W, "Chemical vapor deposition of nickel oxide films from $\text{Ni}(\text{C}_5\text{H}_5)_2\text{O}_2$," *Thin Solid Films*, **2001**, vol. 391, no. 1, pp. 57–61.
20. Liu H., Zheng W., Yan X., and Feng B., "Studies on electrochromic properties of nickel oxide thin films prepared by reactive sputtering," *J. Alloys Compd.*, **2008**, vol. 462, no. 1–2, pp. 356–361.
21. Bruckner W., Kaltofen R., Thomas J., Hecker M., Uhlemann M., Oswald S., Elefant D., and Schneider C.M., "Stress development in sputtered NiO thin films during heat treatment," *J. Appl. Phys.*, **2003**, vol. 94, no. 8, p. 4853.
22. Kuzmin A., Purans J., and Rodionov A., "X-ray absorption spectroscopy study of the Ni K edge in magnetron-sputtered nickel oxide thin films," *J. Phys. Condens. Matter*, **1997**, vol. 9, no. 32, pp. 6979–6993.
23. Itapu S., Borra V. and Mossayebi F., "A computational study on the variation of bandgap due to native defects in stoichiometric NiO and Pd, Pt doping in stoichiometric NiO", *Condensed Matt.*, **2018**, vol. 3, no. 4, 46.
24. Moening J.P. and Georgiev D.G., "Formation of conical silicon tips with nanoscale sharpness by localized laser irradiation," *J. Appl. Phys.*, **2010**, vol. 107, no. 1, p. 14307.
25. Moening J.P., Thanawala S.S., and Georgiev D.G., "Formation of high-aspect-ratio protrusions on gold films by localized pulsed laser irradiation," *Appl. Phys. A*, **2009**, vol. 95, no. 3, pp. 635–638.
26. Lu H., Tu Y., Lin X., Fang B., Luo D., and Laaksonen A., "Effects of laser irradiation on the structure and optical properties of ZnO thin films," *Mater. Lett.*, **2010**, vol. 64, no. 19, pp. 2072–2075.
27. Kim K., Kim S., and Lee S.Y., "Effect of excimer laser annealing on the properties of ZnO thin film prepared by sol-gel method," *Curr. Appl. Phys.*, **2012**, vol. 12, no. 2, pp. 585–588.
28. Gupta P., Dutta T., Mal S., and Narayan J., "Controlled p-type to n-type conductivity transformation in NiO thin films by ultraviolet-laser irradiation," *J. Appl. Phys.*, **2012**, vol. 111, no. 1, p. 13706.
29. Itapu S., Georgiev D.G., Upadhyay P. and Podraza N.J., "Modification of reactively sputtered NiO_x thin films by pulsed laser irradiation", *Phys. Status Solidi (a)*, **2017**, vol. 214, no. 2, 1600414.
30. Abal'oshev A., Abal'osheva I., Gierłowski P., Lewandowski S.J., Konczykowski M., Rizza G., and Chromik Š., "Effect of pulsed UV laser irradiation on the properties of crystalline $\text{YBa}_2\text{Cu}_3\text{O}_{7-\delta}$ thin films," *Supercond. Sci. Technol.*, **2007**, vol. 20, no. 5, pp. 433–440.
31. Chang L., Jiang Y., and Ji L., "Improvement of the electrical and ferromagnetic properties in $\text{La}_{0.67}\text{Ca}_{0.33}\text{MnO}_3$ thin film irradiated by CO_2 laser," *Appl. Phys. Lett.*, **2007**, vol. 90, no. 8, p. 82505.
32. Ji L., Jiang Y., Wang W., and Yu Z., "Enhancement of the dielectric permittivity of Ta_2O_5 ceramics by CO_2 laser irradiation," *Appl. Phys. Lett.*, **2004**, vol. 85, no. 9, pp. 1577–1579.
33. Papernov S., Kozlov A.A., Oliver J.B., Kessler T.J., Shvydky A., and Marozas B., "Near-ultraviolet absorption annealing in hafnium oxide thin films subjected to continuous-wave laser radiation," *Opt. Eng.*, **2014**, vol. 53, no. 12, p. 111 122504.
34. Scorticati D., Illiberi A., Bor T., Eijt S.W.H., Schut H., Römer G.R.B.E., de Lange D.F., and in't Veld A.J.H., "Annealing of SnO_2 thin films by ultra-short laser pulses," *Opt. Express*, **2014**, vol. 22, no. S3, p. A607.
35. Ichikawa Y., Chi H.A., Setsune K., Kawashima S.I., and Kugimura K., "Crystallization of Amorphous Titanium Oxide Thin Films by Pulsed UV-Laser Irradiation," *MRS Proc.*, **1995**, vol. 397, p. 447.
36. Farooq W.A., Al Saud M., and Alahmed Z.A., "Structural and optical properties of laser irradiated nanostructured cadmium oxide thin film synthesized by a sol-gel spin coating method," *Opt. Spectrosc.*, **2016**, vol. 120, no. 5, pp. 745–750.
37. Hong R., Wei C., He H., Fan Z., and Shao J., "Influences of CO_2 laser irradiation on the structure and photoluminescence of zinc oxide thin films," *Thin Solid Films*, **2015**, vol. 485, no. 1–2, pp. 262–266.
38. Liu A., Liu G., Zhu H., Shin B., Fortunato E., Matins R. and Shan F., "Hole mobility modulation of solution-processed nickel oxide thin-film transistor based on high-k dielectric", *Appl. Phys. Lett.*, **2016**, vol. 108, 233506.
39. Shan F., Liu A., Zhu H., Kong W., Liu J., Shin B., Fortunato E., Martins R. and Liu G., "High-mobility p-type NiO_x thin-film transistors processed at low temperatures with Al_2O_3 high-k dielectric", *J. Mater. Chem. C*, **2016**, vol. 4, pp. 9438–9444.

40. Xu W., Zhang J., Li Y., Zhang L., Chen L., Zhu D., Cao P., Liu W., Han S., Liu X. and Lu Y., "p-type transparent amorphous oxide thin-film transistors using low-temperature solution-processed nickel oxide", *J. Alloys & Compounds*, **2019**, vol. 806, pp. 40-51.
41. Shang Z.W., Hsu H.H., Zheng Z.W. and Cheng C.H., "Progress and challenges in p-type oxide based thin film transistors", *Nanotechnol. Rev.*, **2019**, vol. 8, pp. 422-443.